Cardiovascular regulation during sleep quantified by symbolic coupling traces

A. Suhrbier,[1] M. Riedl,[2] H. Malberg,[3] T. Penzel,[4] G. Bretthauer,[1] J. Kurths,[2,5] and N. Wessel[2,a)]
[1]*Institute for Applied Computer Science, Forschungszentrum Karlsruhe GmbH (Karlsruhe Research Center), Karlsruhe Institute of Technology (KIT), Karlsruhe 76131, Germany*
[2]*Department of Physics, Humboldt-Universität zu Berlin, Berlin 10115, Germany*
[3]*Institute of Biomedical Engineering, Dresden University of Technology, Dresden 01187, Germany*
[4]*Sleep Center, Charité University Hospital, Berlin 10117, Germany*
[5]*Potsdam Institute for Climate Impact Research, Potsdam 14473, Germany and Institute for Complex Systems and Mathematical Biology, University of Aberdeen, Aberdeen AB24 3FX, United Kingdom*

(Received 13 August 2010; accepted 1 November 2010; published online 30 December 2010)

Sleep is a complex regulated process with short periods of wakefulness and different sleep stages. These sleep stages modulate autonomous functions such as blood pressure and heart rate. The method of symbolic coupling traces (SCT) is used to analyze and quantify time-delayed coupling of these measurements during different sleep stages. The symbolic coupling traces, defined as the symmetric and diametric traces of the bivariate word distribution matrix, allow the quantification of time-delayed coupling. In this paper, the method is applied to heart rate and systolic blood pressure time series during different sleep stages for healthy controls as well as for normotensive and hypertensive patients with sleep apneas. Using the SCT, significant different cardiovascular mechanisms not only between the deep sleep and the other sleep stages but also between healthy subjects and patients can be revealed. The SCT method is applied to model systems, compared with established methods, such as cross correlation, mutual information, and cross recurrence analysis and demonstrates its advantages especially for nonstationary physiological data. As a result, SCT proves to be more specific in detecting delays of directional interactions than standard coupling analysis methods and yields additional information which cannot be measured by standard parameters of heart rate and blood pressure variability. The proposed method may help to indicate the pathological changes in cardiovascular regulation and also the effects of continuous positive airway pressure therapy on the cardiovascular system. © *2010 American Institute of Physics*.
[doi:10.1063/1.3518688]

Directional coupling analysis of bivariate time series is an important subject of current research. In this paper, a method based on symbolic dynamics[1] for the detection of time-delayed coupling is presented. The symbolic coupling traces (SCT), defined as the symmetric and diametric traces of the bivariate word distribution, allow the quantification of coupling and are compared with established methods such as cross correlation, mutual information, and recurrence analysis. It is applied to coupling analysis of heart rate and systolic blood pressure during sleep. Sleep is not just the absence of wakefulness but has its own internal structure. The internal structure can be described by different sleep stages based on visual pattern classification.[2] It is assumed that these sleep stages modulate the cardiovascular regulation. The cardiovascular consequences of disturbed sleep are of particular high medical interest for sleep physicians because they present a risk factor for cardiovascular disorders such as hypertension, cardiac ischemia, sudden cardiac death, and stroke. Our new derived measures may help to detect pathological mechanisms for these health risks during sleep. Understanding these cardiovascular mechanisms during sleep may be useful to predict the effects of treatment in subjects with disordered breathing during sleep as well as in other sleep disorders and effects of aging in healthy subjects.

I. INTRODUCTION

Biological systems usually consist of several subsystems which are interrelated by feedback loops with time delay. To reveal such time-delayed coupling directions from biosignals is a basic task in understanding such systems.[3–6] Data recorded from these systems reflect the biological activities of living beings and contain real biological information including nonstationarities, nonlinearities, intrinsic noise, and artifacts. Therefore, the analysis of biosignals, especially the detection of coupling directions, is complex. Different methods, starting from cross correlation via mutual predictability to information-theoretic approaches,[7–12] were applied to biosignals. All these methods are able to find directions of interactions. However, due to the nonstationarity and non-

a)Author to whom correspondence should be addressed. Electronic mail: wessel@physik.hu-berlin.de.

TABLE I. Number of data sets for considered groups (C—healthy controls, NT—normotensive patients, HT—hypertensive patients, DD—differential diagnosis night, CPAP—night with CPAP therapy after 3 month CPAP treatment, W—awake state, LS—light sleep, DS—deep sleep, REM—rapid eye movement).

Subjects	Measurement	W	LS	DS	REM
C	DD	7	10	10	10
NT	DD	14	18	18	18
	CPAP	13	14	14	14
HT	DD	8	10	6	8
	CPAP	8	9	9	9

linearity of the biosignals, the conclusions are not homogeneous.

In this paper we take on the problem of analyzing the cardiovascular regulation during different sleep stages, which is a current problem in sleep medicine. In Sec. II we demonstrate the advantage of SCT for coupling analysis by comparing the different methods on simulated data before we apply SCT to real data from the sleep laboratory. Using a new estimation procedure for significant coupling, we quantify the interactions in short-term cardiovascular regulation and calculate the standard frequency and baroreflex parameters as well. In Sec. III we present the results of this comparison and show the different abilities of the methods to quantify the cardiovascular regulation in different sleep stages and between different patient groups. Finally, in Sec. IV we discuss and interpret the results on the basis of physiological mechanisms.

II. MATERIAL AND METHODS

A. Data

For application of SCT, we consider polysomnographic measurements of 18 normotensive (NT) (age: 44.6 ± 7.6 yr, body mass index (BMI): 30.2 ± 2.9 kg/m^2, all male) and 10 hypertensive (HT) patients (age: 44.1 ± 8.1 yr, BMI: 34.1 ± 4.9 kg/m^2, all male) suffering from obstructive sleep apnea syndrome (OSAS) (repetitive obstruction of the upper airway for more then 10 s during sleep) during a diagnostic night [differential diagnosis (DD)] and during treatment by means of continuous positive airway pressure (CPAP) (positive pressure via mask avoids obstructions of the upper airway during apneas). We consider the first 5 min of the largest undisturbed period of light sleep (LS), deep sleep (DS), rapid eye movement (REM), and the awake state (W) for each subject (see Table I). The epochs for some stages were excluded due to artifacts (e.g., only nine hypertensive patients had 5 min of undisturbed LS during CPAP therapy). Additionally, a control group of ten healthy controls (C, age: 44.8 ± 6.7 yr, BMI: 25.3 ± 2.7 kg/m^2, all male) is examined. The polysomnographic recordings include electroencephalogram (EEG), electrooculogram (EOG), electromyogram (EMG), respiratory airflow, electrocardiogram (ECG), and continuous blood pressure curve. EEG, EOG, and EMG are used to divide the sleep into different sleep stages following the protocol of Rechtschaffen and Kales.[2] The respiratory signal indicates disturbances caused by apneas.

For group specific results, the mean and standard deviation of parameters are calculated for each group. From the ECG signal (sampling rate of 1000 Hz) of these periods, the instance of the heartbeats is determined using appropriate algorithms.[13] Intervals between successive heartbeats ($\{B_i\}$—beat-to-beat intervals) are calculated and artifacts caused by, e.g., premature beats were removed in B_i by means of an adaptive filter.[14,15] Additionally, the maximum blood pressure value in each beat-to-beat interval is extracted from the continuous blood pressure (via finger cuff of Portapres device model 2, BMI-TNO, Amsterdam, The Netherlands; sampling rate of 200 Hz), which leads to the time

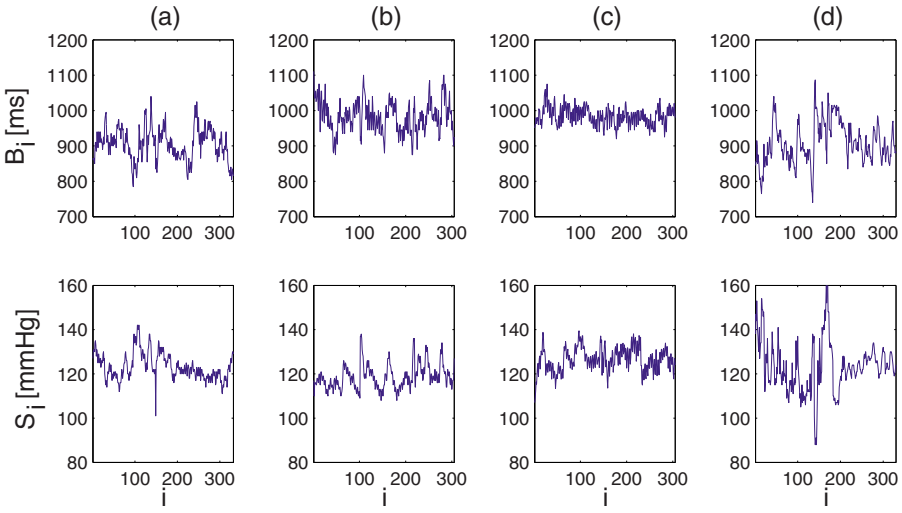

FIG. 1. (Color online) Extracted time series of beat-to-beat interval (B_i) and systolic blood pressure (S_i) for a healthy subject during different sleep stages [wake—column (a); light sleep—column (b); deep sleep—column (c); and REM sleep—column (d)].

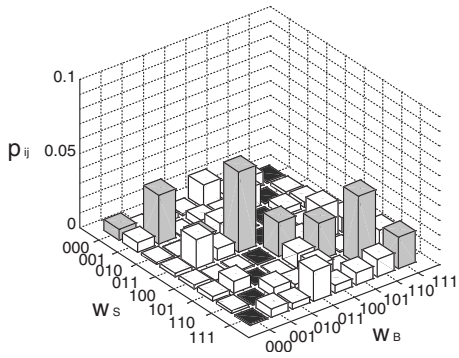

FIG. 2. Schematic illustration of the symbolic coupling traces. Each diagonal of the bivariate word distribution represents symmetric and diametric behavior in the signals, respectively.

series of systolic blood pressure on beat-to-beat basis ($\{S_i\}$—systolic blood pressure). Examples are shown in Fig. 1.

B. Symbolic coupling traces

For bivariate coupling analysis we used SCT.[16] The first step of this approach is the transformation of B_i and S_i into symbol sequences $s_B(t)$ and $s_S(t)$ according to the rule,

$$s_z(t) = \begin{cases} 1 & z(t) \leq z(t+\theta) \\ 0 & z(t) > z(t+\theta), \end{cases} \tag{1}$$

where z represents B and S. For analysis of short-term couplings in B_i and S_i, the value $\theta=1$ has been used.[16] Next, words of length l are constructed $w_z(t) = s(t), s(t+1), \ldots, s(t+l-1)$ which can form $d=2^l$ different patterns. For short-term dynamics in B_i and S_i, $l=3$ is used to reliably estimate the bivariate word distribution.[16] $w_x(t)$ and $w_y(t)$ are used to calculate the bivariate word distribution $(p_{ij})_{i=1,\ldots,d,j=1,\ldots,d}(\tau)$,

$$p_{ij}(\tau) = P(w_x(t) = W_i, w_y(t+\tau) = W_j), \tag{2}$$

with the d patterns W_1 to W_d (see Fig. 2). The parameter τ is included in order to consider delayed interrelationships between the signals. From the bivariate word distribution, the parameters

$$T = \sum_{i=j} p_{ij}(\tau), \tag{3}$$

$$\bar{T} = \sum_{i=1,\ldots,d;j=d+1-i} p_{ij}(\tau), \tag{4}$$

$$\Delta T = T - \bar{T} \tag{5}$$

are calculated. On the one hand, T only captures influences which preserve the structure of the transmitted pattern of dynamics (symmetrical influences). On the other hand, $\bar{T}$ only quantifies influences which inverts the dynamical structure of the driver (diametrical influence).

To answer the question if the parameters T and $\bar{T}$ are significant or not, a critical value T_{crit} is estimated, respectively. Therefore, these parameters are calculated for 1000 realizations of bivariate white noise $N_i(0,\sigma^2)$ with sample length N. In the case of T and $\bar{T}$, we look for the 99th percentile where 99% of the 1000 observations are smaller than that value. It represents the critical value of the significance level $\alpha=0.01$ in a one-side significance test. The pairs of simulated time series are not shifted because the elements of the white noise process are independent from each other. This leads to the same critical values for each delay. For a fast estimation of these critical values, the dependency of these limits on N is estimated by means of regression formula. An example for $T_{\text{crit}}(N)$ is shown in Fig. 3. The formula of this dependency is given in Table II, not only for ΔT but also for the alternative methods introduced in the next paragraph.

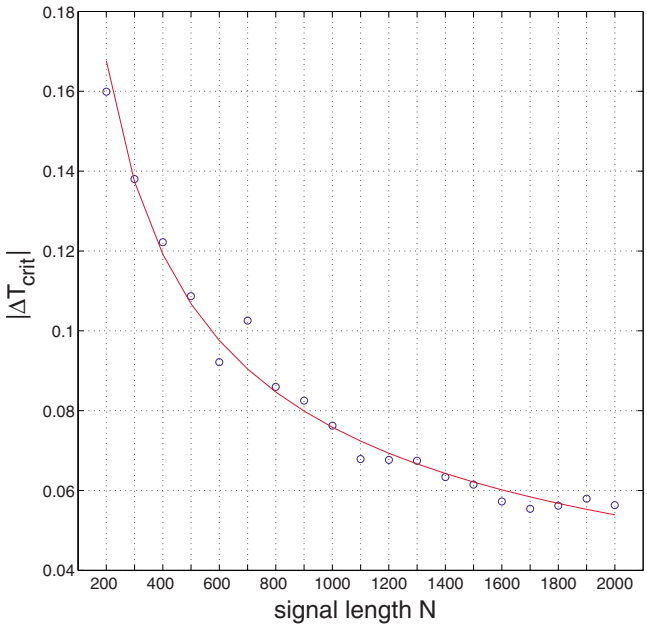

FIG. 3. (Color online) Critical value of ΔT [see Eq. (5)] depending on the length of time series N (correspondent significance level $\alpha=0.01$). The fitted power law is shown by the curve ($\Delta T_{\text{crit}} \approx \pm 2.7005 \cdot N^{-0.5179}$).

C. Alternative measures

Apart from the SCT parameters, the classic cross correlation function (R), mutual information (I), and cross recurrence analysis (ΔRR) are calculated for the differentiated signals as well in order to maintain the comparison to the SCT results.

For the validation of these coupling measures, the simplest approach is used: simulations of coupled two-dimensional (autoregressive (AR) processes (cf. Fig. 4, left panel). The coefficients of the AR models are varied in order

TABLE II. The critical value of the parameter p depending on the sample length N which corresponds to a significance level $\alpha=0.01$.

Parameter p	Critical value of p
ΔT	$p_{\text{crit}} \approx \pm 2.7 \cdot N^{-0.51}$
R	$p_{\text{crit}} \approx \pm 2.6 \cdot N^{-0.51}$
I	$p_{\text{crit}} \approx 58.1 \cdot N^{-1.11}$
ΔRR	$p_{\text{crit}} \approx \pm 0.4 \cdot N^{-0.11}$

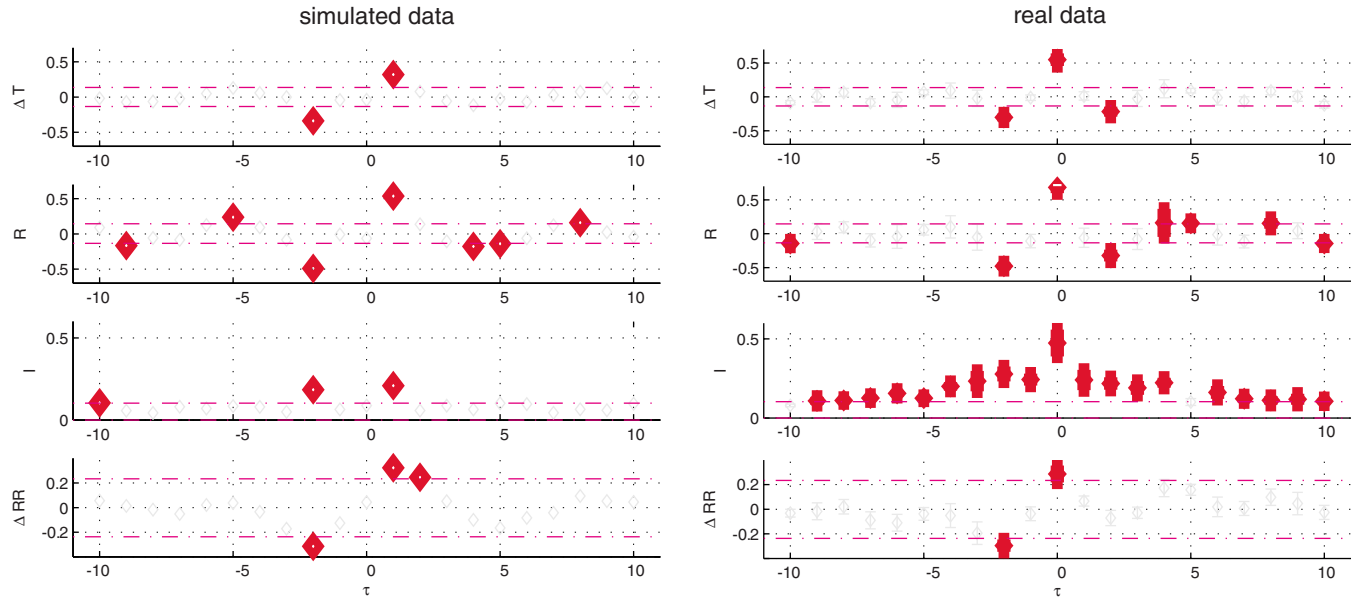

FIG. 4. (Color online) Comparison of different methods: symbolic coupling traces ΔT, cross correlation R, mutual information I, and cross recurrence quantification analysis with order patterns ΔRR for a simulation (left) and normotensive patients without therapy during deep sleep (right) at different lags τ. The simulation was calculated with symmetric coupling at $\tau=1$ as well as diametric coupling at $\tau=-2$ ($x_i=a\cdot x_{i-1}+b\cdot y_{i+1}+\epsilon_i$ and $y_i=c\cdot y_{i-1}+d\cdot x_{i-2}+\nu_i$, two coupling terms y_{i+1} and x_{i-2}; $\epsilon=N(0,0.1)$, $a=0.3$, $b=0.7$, $c=0.3$, $d=0.7$). SCT was able to localize the simulated lags better than the other methods. Cross correlation and mutual information are not very specific, where by ΔRR and ΔT both detect lags 0 and −2. In real data from the diametric lag, +2 represents regular deep breathing during deep sleep and was not detected by ΔRR.

to study the influence of varying coupling strengths and noise. For the example given in Fig. 4 (left panel) with predefined lags at $\tau=-2$ and $\tau=1$, all four methods determine the lags correctly. In contrast to the SCT, however, the other three methods have additional false detections. The SCT-parameter detected the lags in case of delayed coupling with autocorrelation more clearly than cross correlation, mutual information, and cross recurrence quantification analysis based on order pattern (cf. Fig. 4, left panel). For a further validation, we also applied it to nonlinear coupled models, e.g., self-exciting threshold autoregressive model with external input systems,[17] and found similar results.

For a better interpretation of the results, linear parameters of the beat-to-beat and blood pressure variability are considered.[18] The mean value and standard deviation of time domain parameter as well as high frequency and low frequency components of the power spectra of the signals are considered. On one hand, the mean value is associated with the state of the cardiovascular system, which is mainly influenced by the long-term regulation of the neuroendocrine system. On the other hand, standard deviation as well as frequency components reflect the dynamics of the cardiovascular measurements. The power of the high frequency (HF) component, in the range of 0.15–0.4 Hz, reflects the respiratory influence as well as the very fast autonomic regulation via parasympathetic nervous system. The power of the low frequency (LF) component, in the range of 0.04–0.15 Hz, reflects the autonomic regulation of the antagonists parasympathetic and sympathetic nervous system. This autonomic regulation of the opponent vegetative systems acts in the time range of hundreds of milliseconds to several seconds and is called short-term regulation. It is part of control loops which connect the cardiovascular measurements to each other. The baroreflex is a prominent example of this mechanism. It protects the body from sudden dramatical blood pressure changes by regulation of beat-to-beat intervals and peripheral resistance of the vessels and is quantified by the baroreflex sensitivity (BRS). BRS is estimated by means of sequence method where the slope of simultaneously rising of beat-to-beat intervals and blood pressure as well as falling is estimated.[19] To quantify the influence of a 3 month CPAP therapy on the cardiovascular regulation, these standard parameters (partly shown in Table III) are compared before and after using the Kruskal–Wallis test.

III. RESULTS

As introduced in Ref. 16, the SCT results are compared to other standard methods such as R, I, and ΔRR by means of linear as well as nonlinear autoregressive models (see Fig. 4). In contrast to Ref. 16 in this paper, R and I are calculated also for differential time series to have a more appropriate comparison. Nevertheless, both parameters still have problems to detect time-delayed couplings in oscillating signals with noise interaction which results in additional coupling terms, as seen in Fig. 4. ΔRR is only able to produce similar results in the simulation of Fig. 4; however, it shows one false coupling and is computationally very intensive. For real data, we see a similar picture: R and I detecting too many lags, whereas the SCT and ΔRR consistently detect the lags 0 and −2. In addition, the SCT detects also lag +2 for that example of deep sleep.

For all groups and for all sleep stages, we obtain the same characteristic pattern of $\tau=-2$ for diametric coupling ($\bar{T}$) and $\tau=0$ for symmetric coupling (T), as one can see in Fig. 5. Moreover, there are additional lags in light and deep

TABLE III. Mean and standard deviation (mean ± std) of high frequency component of B_i and S_i (HF-B, HF-S; $0.15 \leq f \leq 0.4$ Hz), low frequency component of B_i and S_i (LF-B, LF-S; $0.04 \leq f \leq 0.15$ Hz), and baroreceptor sensitivity (BRS) for healthy controls (C) and NT and HT patients suffering from OSAS during night (DD) as well as treatment by means of CPAP. For testing, a Kruskal–Wallis test is used.

		NT OSAS		HT OSAS		C
Sleep stage	Parameter	DD	CPAP	DD	CPAP	DD
W	HF-B	20.38 ± 13.28	62.97 ± 146.52	8.44 ± 6.36 [a]	15.23 ± 23.25	20.75 ± 16.59
	LF-B	72.79 ± 84.72	89.47 ± 167.56	44.17 ± 54.03 [a]	32.46 ± 40.17	33.43 ± 10.19
	HF-S	**0.21 ± 0.12** [a]	0.26 ± 0.27	0.14 ± 0.08	0.21 ± 0.17	0.18 ± 0.11
	LF-S	**0.64 ± 0.40** [a]	0.91 ± 1.02	0.93 ± 0.95	0.55 ± 0.38	0.74 ± 0.45
	BRS	11.19 ± 3.56	10.42 ± 3.77	8.87 ± 2.40	9.27 ± 3.32	11.44 ± 2.26
LS	HF-B	46.43 ± 46.78	42.79 ± 66.49	37.1 ± 26.90	20.16 ± 17.89	40.80 ± 43.73
	LF-B	108.95 ± 120.88	75.81 ± 66.14	142.21 ± 121.11 [b]	36.92 ± 28.65	74.67 ± 85.31
	HF-S	**0.6 ± 0.67** [c,b]	0.1 ± 0.11	0.35 ± 0.21 [b]	0.1 ± 0.08	0.24 ± 0.28
	LF-S	1.78 ± 2.58	0.89 ± 1.14	1.61 ± 1.22 [b]	0.56 ± 0.53 [c]	1.32 ± 1.01
	BRS	**9.26 ± 2.66** [b]	12.64 ± 3.95	9.88 ± 1.96	11.24 ± 3.70	11.49 ± 3.49
DS	HF-B	35.37 ± 35.30	45.99 ± 87.22	33.22 ± 19.04	16.97 ± 14.23	29.91 ± 28.89
	LF-B	42.78 ± 38.04	55.19 ± 81.62	33.09 ± 31.92	51.23 ± 95.74	41.03 ± 33.30
	HF-S	**0.65 ± 0.51** [c,b]	0.12 ± 0.10	0.77 ± 0.68 [b]	0.14 ± 0.16	0.26 ± 0.24
	LF-S	0.64 ± 0.59	0.46 ± 0.42	1.84 ± 3.33	0.59 ± 0.68	0.61 ± 0.40
	BRS	7.68 ± 3.23	11.38 ± 3.83	6.87 ± 1.72 [b]	10.76 ± 3.85	11.02 ± 3.70
REM	HF-B	29.57 ± 44.61	42.30 ± 106.72	33.08 ± 51.98	15.21 ± 13.29	42.15 ± 58.62
	LF-B	60.84 ± 44.32	95.84 ± 192.31	170.48 ± 280.99	62.96 ± 39.73	127.07 ± 159.03
	HF-S	0.24 ± 0.19	0.17 ± 0.27 [c]	0.29 ± 0.22	0.10 ± 0.07 [c]	0.24 ± 0.18
	LF-S	1.17 ± 0.83	0.76 ± 0.78 [c]	2.08 ± 2.85	1.10 ± 0.73	2.20 ± 2.79
	BRS	9.73 ± 3.60	10.85 ± 3.58	9.25 ± 2.74	10.87 ± 3.10	10.34 ± 4.09

[a]Significant differences between sleep stages within the patient groups ($p < 0.05$).
[b]Significant differences between DD and CPAP ($p < 0.05$).
[c]Significant differences between patient groups NT/HT and C, respectively ($p < 0.05$).

sleep which reach −8 to +4. The hypertensive DD group was the only group with other detected lags beside 0 and −2 in the wake and REM stages [Fig. 5, wake (d)]. As quantified by the Kruskal–Wallis test, there are significant differences in the strength of the detected lags 0 and −2 (stars in Fig. 5). The most prominent difference can be seen between REM and deep sleep, except in the NT CPAP group, Fig. 5(c).

Considering the standard parameters presented in Table III, we obtain the following results. There are significant differences between the sleep stages in the parameters HF-S and LF-S in the normotensive DD group as well as in HF-B and LF-B in the hypertensive DD group ($p < 0.05$, Kruskal–Wallis test). Interestingly, these differences are not present under CPAP therapy and in healthy controls, pointing to sleep disturbances such as snoring and/or apneas as the main cause for these differences. In the normotensive group, differences between the DD and the therapy CPAP night can be detected for HF-S in light and deep sleep as well as BRS in light sleep. For the normotensive group, differences are present for HF-S in light and deep sleep, for LF-B and LF-S in light sleep, as well as for BRS in deep sleep. Comparisons of patient groups with the control group show significant differences in HF-S, light and deep sleep (NT DD versus C), in HF-S, LF-S during REM (NT CPAP versus C), as well as in LF-S during light sleep and HF-S during REM (HT CPAP versus C).

Finally, we consider the more technical results of this paper which deal with a faster calculation of coupling measures. The dependency between the critical values of the coupling parameters ΔT, R, I, and ΔRR and the time series' length N is given by power laws and can be estimated by the formulas noted in Table II. Using these relationships, the calculation of surrogates each time can be avoided.

IV. DISCUSSION

The time-delayed coupling analysis of the theoretical models and our measurements demonstrates the advantage of the SCT in comparison to standard methods. We confirm the results of Ref. 16 where SCT detects significant lags at $\tau = -2$ and $\tau = 0$ for all subjects. This strengthens the prevailing opinion about the cardiovascular short-term regulation. The symmetric lag at $\tau = 0$ reflects the respiratory induced arterial pressure and heart rate fluctuations, whereas the diametric lag at $\tau = -2$ represents the vagal feedback from B_i to S_i. Moreover, we show that this coupling pattern does not change generally in different sleep stages; however, the strength of interactions may differ. During deep sleep only, we see a loss of heart rate and blood pressure asymmetry as well as an effect of CPAP therapy on the cardiovascular coupling.

In this paper, we demonstrate that the SCT is more specific than the standard methods regarding the detection of delays and directions of interactions. In Ref. 16, we applied the cross correlation, mutual information, and the cross recurrence analysis to the original simulated time series. Here we applied them, for a better comparability, to the differentiated time series and still obtain false lags. We assume that

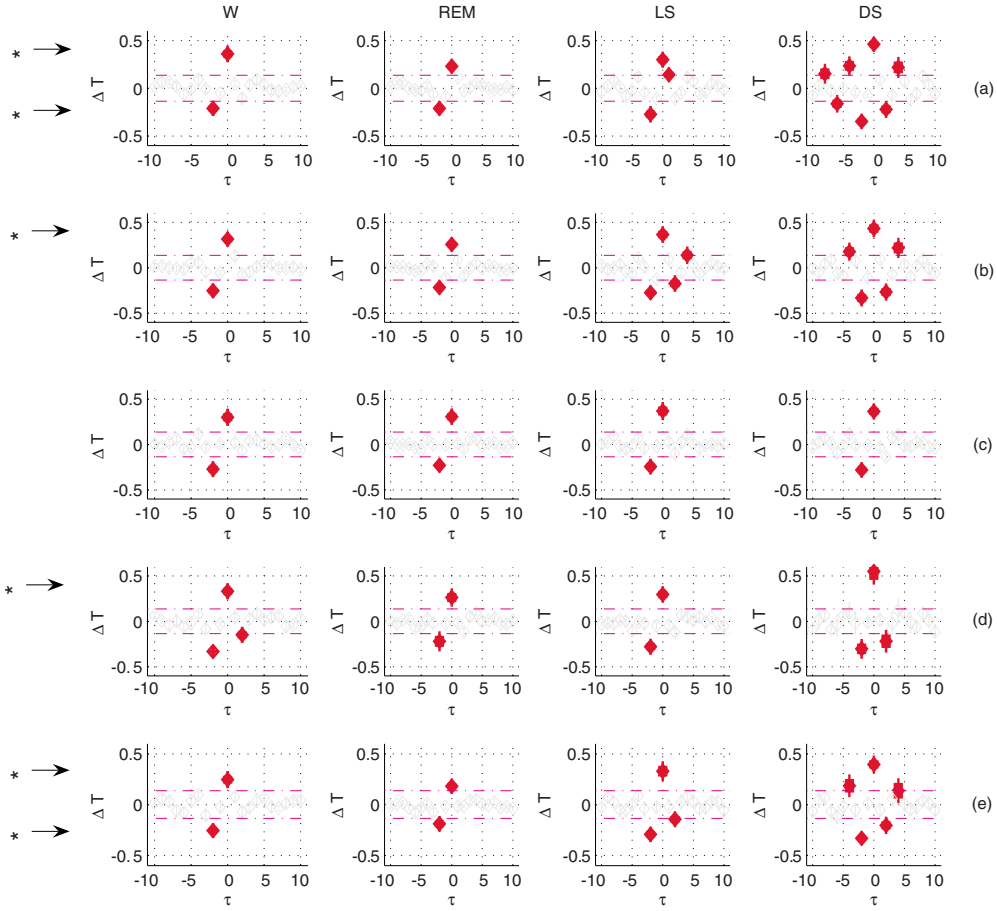

FIG. 5. (Color online) The comparison between the sleep stages (wake=W, REM−sleep=REM, light sleep=LS, deep sleep=DS) and the different patient groups [healthy controls (a), NT DD (b), NT CPAP (c), HT DD (d), HT CPAP (e)] clearly shows the short-term asymmetry in the coupling during wake and REM characterized by lags $\tau=-2$ and $\tau=0$. This asymmetry becomes less in light sleep and is lost in deep sleep when periodic breathing leads to a modulation of B_i and S_i. Significant differences in the coupling strength at $\tau=0$ and $\tau=-2$ between the sleep stages are indicated by (a) ($p<0.05$, Kruskal–Wallis test). Differences exist at both lags in the control patients group as well as HT CPAP. In NT DD and HT DD, only the lag $\tau=0$ is significantly different between the sleep stages.

these methods are more sensitive to nonstationarities, nonlinearities, and noise. Nevertheless, for the general assessment of coupling directions in time series, both new and established methods should be used. Coupling in stationary data with strong noise can be well detected via mutual information and cross correlation, whereas in deterministic data cross recurrence should be preferred. The parameters of the SCT method and cross recurrence based on order pattern close the gap in the coupling analysis of nonstationary time series with strong autocorrelation and moderate noise, where cross correlation, mutual information, and other methods are not sufficient to localize the lags exactly.

The prevailing opinion about the cardiovascular short-term regulation is based on antagonistic nervous control via vagus and sympathicus. Here, we confirm the results of Ref. 16 with significant lags at $\tau=-2$ and $\tau=0$. Moreover, we show that this coupling pattern does not change generally in different sleep stages; however, the strength of interactions may differ. The highest amplitudes for ΔT we find for deep sleep, the lowest for REM (cf. Fig. 5). This relation can be explained with a reduced sympathetic activity during deep sleep as quantified by LF-B in Table III,[20] leading to more pronounced respiratory influence and an increased vagal feedback. Again, during deep sleep, where many physiological regulatory mechanisms such as cerebral blood flow and cerebral metabolic rate are reduced,[21] we find an increased heart rate and blood pressure symmetry leading to multiple lags of $\tau=-2$ and $\tau=0$. It shows a limitation of the coupling traces for symmetric oscillations, but this is a limitation of all methods for the detection of coupling directions.

Considering the CPAP therapy, we see that there are no different coupling patterns before and after treatment during the wake and the REM state. However, during deep sleep, we see clear differences in the cardiovascular couplings (Fig. 5). These results are confirmed by the parameters of heart rate and blood pressure variability (see Table III), mainly by HF-S, which reflects the mechanical effects of respiration on blood pressure:[22] the higher the HF-S, the higher the respiratory effort. The influence of the CPAP device on systolic blood pressure variations is obvious for all sleep stages, except wake. The baroreflex sensitivity shows no consistent effects for all sleep stages regarding the CPAP therapy. We see significant improvements during light sleep in the normotensive group and during deep sleep in the hypertensive group, which confirms the results of Ref. 23 where mean BRS increased only slightly during CPAP application. By

comparing the significant differences in the standard parameters and the results of SCT analysis before and after CPAP therapy in light and deep sleep, we can conclude that the coupling information is independent of the variability parameters.

In summary, the proposed method of the symbolic coupling traces may help to indicate the pathological changes in cardiovascular regulation and also the effects of continuous positive airway pressure therapy on the cardiovascular system.

ACKNOWLEDGMENTS

This work was supported by the German Science Foundation (Grant Nos. DFG KU837/23-1, DFG PE 628/4-1, and BR1303/10-1).

[1]A. Voss, J. Kurths, H. J. Kleiner, and N. Wessel, J. Electrocardiol. **28**, 81 (1995).
[2]*A Manual of Standardized Terminology, Techniques and Scoring System for Sleep Stages of Human Subjects*, edited by A. Rechtschaffen and A. Kales (U.S. Government Printing Office, Washington, DC, 1968).
[3]B. Blasius, A. Huppert, and L. Stone, Nature (London) **399**, 354 (1999).
[4]L. Glass, Nature (London) **410**, 277 (2001).
[5]U. Feldmann and J. Bhattacharya, Int. J. Bifurcation Chaos Appl. Sci. Eng. **14**, 505 (2004).
[6]P. Van Leeuwen, D. Geue, M. Thiel, D. Cysarz, S. Lange, M. Romano, N. Wessel, J. Kurths, and D. Grönemeyer, Proc. Natl. Acad. Sci. U.S.A. **106**, 13661 (2009).
[7]B. Schelter, M. Winterhalder, R. Dahlhaus, J. Kurths, and J. Timmer, Phys. Rev. Lett. **96**, 208103 (2006).
[8]L. Faes, A. Porta, and G. Nollo, Phys. Rev. E **78**, 026201 (2008).
[9]N. Marwan, M. C. Romano, M. Thiel, and J. Kurths, Phys. Rep. **438**, 237 (2007).
[10]M. Paluš and A. Stefanovska, Phys. Rev. E **67**, 055201 (2003).
[11]T. Schreiber, Phys. Rev. Lett. **85**, 461 (2000).
[12]M. Staniek and K. Lehnertz, Phys. Rev. Lett. **100**, 158101 (2008).
[13]A. Suhrbier, R. Heringer, T. Walther, H. Malberg, and N. Wessel, Biomed. Tech. **51**, 70 (2006).
[14]N. Wessel, A. Voss, H. Malberg, C. Ziehmann, H. U. Voss, A. Schirdewan, U. Meyerfeldt, and J. Kurths, Herzschrittmacherther. Elektrophysiol. **11**, 159 (2000).
[15]N. Wessel, H. Malberg, R. Bauernschmitt, and J. Kurths, Int. J. Bifurcation Chaos Appl. Sci. Eng. **17**, 3325 (2007).
[16]N. Wessel, A. Suhrbier, M. Riedl, N. Marwan, H. Malberg, G. Bretthauer, T. Penzel, and J. Kurths, EPL **87**, 10004 (2009).
[17]H. Tong, *NonLinear Time Series: A Dynamical System Approach* (Oxford University Press, Oxford, 1990).
[18]Task Force of the European Society of Cardiology, the North American Society of Pacing, and Electrophysiology, Circulation **93**, 1043 (1996).
[19]H. Malberg, N. Wessel, A. Hasart, K. J. Osterziel, and A. Voss, Clin. Sci. **102**, 465 (2002).
[20]S. Akselrod, D. Gordon, F. A. Ubel, D. C. Shannon, A. C. Barger, and R. J. Cohen, Science **213**, 220 (1981).
[21]P. Madsen and S. Vorstrup, Cerebrovasc Brain Metab. Rev. **3**, 281 (1991).
[22]G. Parati, J. P. Saul, M. D. Rienzo, and G. Mancia, Hypertension **25**, 1276 (1995).
[23]M. Bonsignore, G. Parati, G. Insalaco, P. Castiglioni, O. Marrone, S. Romano, A. Salvaggio, G. Mancia, G. Bonsignore, and M. D. Rienzo, Eur. Respir. J. **27**, 128 (2006).